A Sequence Component Based Continuation Power Flow Model for Electric Power Grid Considering Transmission and Distribution System

Arun Suresh, *Member, IEEE,* Sumit Paudyal, *Member, IEEE,* and Sukumar Kamalasadan, *Senior Member, IEEE*

***Abstract*—Integration of Inverter Based Resources (IBRs) in the distribution grid and bulk grid has posed new challenges to the long-term voltage stability of the integrated electric Transmission and Distribution (T&D) system. The main challenges include, but are not limited to, IBR variability and intermittence, the effect of a large number of DERs, distribution grid unbalances, the effect of load types, and the interaction of controllable devices such as voltage regulators. This paper proposes a new three-sequence integrated T&D continuation power flow (SI-CPF) model for analyzing the voltage stability of the power grid considering, grid and load unbalance, various load types, and renewable energy variations, in a combined T&D simulation that consider all the phases of transmission and distribution network. Results show that SI-CPF can provide the weak phase voltage stability margin of the power grid more efficiently and accurately considering a three-phase integrated T&D network.**

***Index Terms*—Integrated Transmission and Distribution Sequence Continuation Power Flow (SI-CPF), Voltage Stability Analysis, Inverter Based Resources (IBRs), T& D Co-Simulation, Sequence Components.**

I. Introduction

MODERNIZATION of the electric distribution grid with several distributed generators, energy storage and Electric Vechicles (EVs) provides a need to perform transmission system analysis taking into account detailed variations at the distribution level. Towards this end, an integrated grid modeling approach is needed for the accurate analysis of the electric grid with smart energy resources. This paper proposes an SI-CPF model that captures characteristics of transmission and distribution systems together, considering factors like reverse power flow with unbalanced conditions, and simulating the entire power system as a unified environment.

State-of-the-art power flow and stability studies models a positive sequence representation of transmission and distribution systems. Recently an integrated T&D modeling approach was introduced in (decoupled method and unified method) [1] in positive sequence domain for the transmission and single-phase representation for distribution system for solving integrated system were studied. Thus the impact of sequence representation from single phase developed model inaccuracies. In [2], T&D models are developed with transmission system represented in three-sequence framework and distribution system in three-phase. This presentation takes into acount the distribution system unbalances however, did not include IBR related resources. In [3], a dynamic model of a combined T& D is presented including Inverter Based Resources (IBR) dynamics. Ref. [4], [5] and [6] introduces the impact of photovoltaics (PV) from secondary distribution networks on integrated T&D models including scalability. Two commercial-grade platforms that can run the T &D models include the Distributed Engineering Workstation (DEW) [7] and the Hierarchical Engine for Large-scale Infrastructure Co-Simulation (HELICS) [8]. Due to the non-compatibility of power-flow models, the transmission system power-flow modeling may not be suitable for distribution networks. Ref. [9] and [10] introduces methods for voltage stability analysis of the integrated T&D co-simulation where the transmission system is modeled in the sequence domain. In our earlier work, [11], we have demonstrated that the accurate models to assess the voltage stability margin are when developing models for transmission systems in three-phase compared to sequence representation [12]. Similarly, in [13], an unbalanced continuation power flow model is developed in the three-phase domain for the unbalanced electric distribution system.

This paper proposes a novel three-sequence-based continuation power flow method that is computationally faster than three-phase approaches. The main contributions include a) an unbalance integrated T&D modeling approach with detailed models of all devices lines, voltage regulators transformers and load types and b) sequence representation with accurate voltage profile dynamic representation providing insights on voltage stability margin. As for paper organization, Section II summarizes the different transmission and distribution system models required for the continuation power flow analysis. The proposed unified T&D Modeling is discussed in Section III. Section IV introduces the integrated T&D Power Flow Model and section V extends it to the proposed integrated T&D Continuation Power Flow model. Section VI discusses simulation results. Conclusions and future works are discussed in Section VII.

II. Power Transmission and Distribution System Modeling

In the proposed model, first, a bus admittance matrix considering all the device models are developed based on work in [14] as

$$\underbrace{\begin{bmatrix} Y_{11}^{abc} & Y_{12}^{abc} & \cdots & Y_{1N}^{abc} \\ Y_{21}^{abc} & Y_{22}^{abc} & \cdots & Y_{2N}^{abc} \\ \vdots & \vdots & \ddots & \vdots \\ Y_{N1}^{abc} & Y_{N2}^{abc} & \cdots & Y_{NN}^{abc} \end{bmatrix}}_{Y_D^{abc}} \begin{bmatrix} \mathbf{V}_1^{abc} \\ \mathbf{V}_2^{abc} \\ \vdots \\ \mathbf{V}_N^{abc} \end{bmatrix} = \begin{bmatrix} \mathbf{I}_1^{abc} \\ \mathbf{I}_2^{abc} \\ \vdots \\ \mathbf{I}_N^{abc} \end{bmatrix} \tag{1}$$

where Y_{ii}^{abc} represents the self-admittance of bus i and Y_{ij}^{abc} represents the mutual-admittance between bus i and j, both

Partial support for this research is provided through the Solar Energy Technologies Office Award Number DE-EE0008774 by the U.S. Department of Energy's Office of Energy Efficiency and Renewable Energy (EERE), as well as the National Science Foundation grants ECCS-1810174 and ECCS-2001732. Corresponding Author: Sukumar Kamalasadan, Email: skamalas@uncc.edu

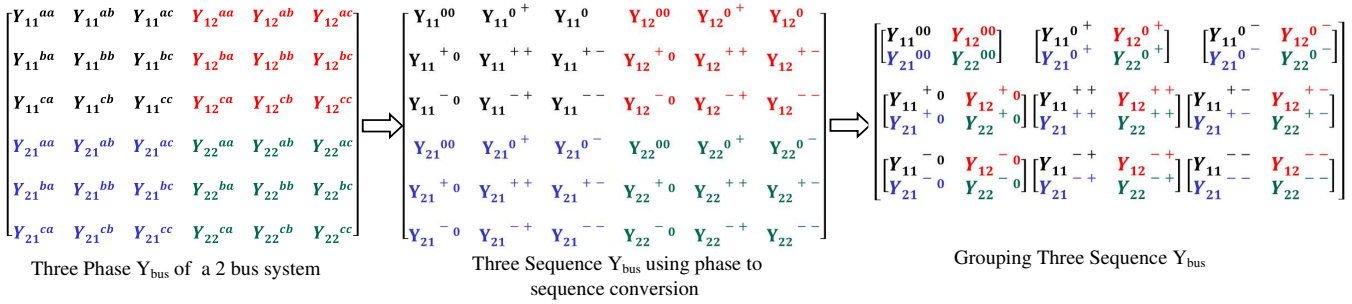

Fig. 1. Formation of sequence admittance matrix.

in a 3x3 submatrix form. To obtain sequence admittance submatrices from each of the phase admittance submatrices in (1), the following conversion is performed

$$Y_{ii}^{012} = C^{-1} Y_{ii}^{abc} C \tag{2}$$

where

$$C = \begin{bmatrix} 1 & 1 & 1 \\ 1 & a^2 & a \\ 1 & a & a^2 \end{bmatrix} \tag{3}$$

where $\mathbf{a} = \mathbf{1} < 120 \qquad \mathbf{a}^2 = \mathbf{1} < 240$

For example, with a three-phase network with two buses, the phase admittance matrix will be a 6×6 matrix and the grouped sequence submatrices can be represented as shown in Fig. 1 which can be written as

$$Y_D^{0+-} = \begin{bmatrix} Y_D^{00} & Y_D^{0+} & Y_D^{0-} \\ Y_D^{+0} & Y_D^{++} & Y_D^{+-} \\ Y_D^{-0} & Y_D^{-+} & Y_D^{--} \end{bmatrix} \tag{4}$$

Similarly, the bus admittance matrix of a transmission system in sequence component frame is represented as as

$$Y_T^{0+-} = \begin{bmatrix} Y_T^{00} & 0 & 0 \\ 0 & Y_T^{++} & 0 \\ 0 & 0 & Y_T^{--} \end{bmatrix} \tag{5}$$

Since the transmission system consists of transposed lines, the mutual components in the sequence admittance matrix will be zero.

To represent loads, constant-current, constant-power, and constant-impedance load model (ZIP) has been used. The net nodal current injection based on ZIP load model is given by

$$(I_i^{sp})^s = -\left[\left(\frac{|S_i^s|\angle\theta^s}{|V_i^s|\angle\delta^s}\right)^* + \left(\frac{|S_i^s|}{|V_{0i}^s|}\right)\angle(\delta^s - \theta^s) + \left(\frac{V_i^s}{Z_i^s}\right)\right] \tag{6}$$

where δ, θ, V_{0i} is the voltage angle, power factor angle and the nominal voltage respectively. S_i^s is scheduled power and Z_i is the impedance of the load.

III. Proposed Unified T&D Modeling

The proposed method utilizes a unified transmission and distribution co-simulation approach which treats the T&D network as a one system and solves it using one method as shown in Fig. 2.

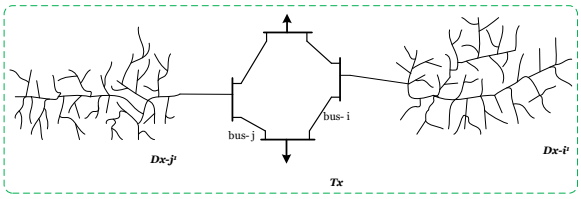

Fig. 2. Integrated unified T&D one line diagram.

A. Stacked Unified Ybus

The stacked Ybus approach in three-sequence bus admittance representation involves grouping based on sequences. The approach utilizes three vectors viz. the Starting Bus Vector (**SBV**), the Position Vector (**PV**) and the Tie Line Vector (**TLV**) and creates a renumbered unified T&D system. The starting buses of all distribution networks are captured in **SBV**, while the **PV** contains the starting buses and total bus count of each distribution network. The **TLV** has 2 columns, with the first column representing the starting bus of a distribution network and the second column representing the transmission bus to which that distribution network gets connected.

The stacked Ybus approach is demonstrated using an example in Fig. 3(b). The **SBV**, **PV**, and **TLV** matrices can

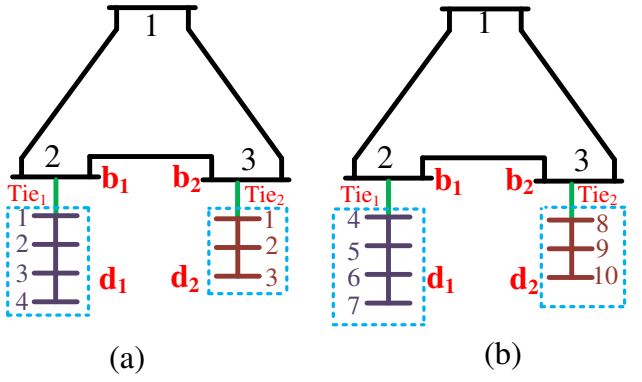

Fig. 3. (a) Unifed T&D one-line (b) Renumbered T&D One-line.

be written as

$$\mathbf{SBV} = \begin{bmatrix} 4 \\ 8 \end{bmatrix} \mathbf{PV} = \begin{bmatrix} 4 & 4 \\ 8 & 3 \end{bmatrix} \mathbf{TLV} = \begin{bmatrix} 4 & 2 \\ 8 & 3 \end{bmatrix} \tag{7}$$

Let the total number of transmission buses be n_t, that of distribution networks 1 and 2 be n_{d1} and n_{d2} respectively and n_T

be the total buses in the unified system. The positive sequence Ybus of the transmission network, distribution network 1, and distribution network 2 are denoted as $\boldsymbol{Y_T^{++}}$, $\boldsymbol{Y_{D1}^{++}}$, and $\boldsymbol{Y_{D2}^{++}}$, respectively, and are defined as

$$\mathbf{Y_T^{++}} = \begin{bmatrix} y_t^{11} & y_t^{12} & y_t^{13} \\ y_t^{21} & y_t^{22} & y_t^{23} \\ y_t^{31} & y_t^{32} & y_t^{33} \end{bmatrix} \mathbf{Y_{D1}^{++}} = \begin{bmatrix} y_{d1}^{11} & y_{d1}^{12} & y_{d1}^{13} & y_{d1}^{14} \\ y_{d1}^{21} & y_{d1}^{22} & y_{d1}^{23} & y_{d1}^{24} \\ y_{d1}^{31} & y_{d1}^{32} & y_{d1}^{33} & y_{d1}^{34} \\ y_{d1}^{41} & y_{d1}^{42} & y_{d1}^{43} & y_{d1}^{44} \end{bmatrix}$$

$$\mathbf{Y_{D2}^{++}} = \begin{bmatrix} y_{d2}^{11} & y_{d2}^{12} & y_{d2}^{13} \\ y_{d2}^{21} & y_{d2}^{22} & y_{d2}^{23} \\ y_{d2}^{31} & y_{d2}^{32} & y_{d2}^{33} \end{bmatrix} \tag{8}$$

To obtain the unified positive sequence admittance matrix, a zero matrix $\boldsymbol{Y_U}$ with size of n_T x n_T is used. $\boldsymbol{Y_T^{++}}$ is stacked over the first n_t x n_t portion of $\boldsymbol{Y_U}$. The rest of $\boldsymbol{Y_U}$ is populated using $\mathbf{PV}$ matrix, traversing through each row. The Ybus of the unified system at this point does not include the values for tie lines connecting the T&D systems. To account for this, a tie line correction step is carried out using the $\mathbf{TLV}$ matrix by traversing through each row. In this example values corresponding to $\boldsymbol{Y^U(2,2)}$,$\boldsymbol{Y^U(4,4)}$,$\boldsymbol{Y^U(2,4)}$,$\boldsymbol{Y^U(4,2)}$, is updated for tie line correction of distribution system 1. The positive sequence unified Ybus $\boldsymbol{Y_{TD}^{++}}$ is obtained as (9). This procedure is repeated to obtain the negative sequence, zero sequence self-admittance matrices (Y^{--}, Y^{00}) and mutual admittance matrices (Y^{0+}, Y^{0-}, Y^{+-}). The three sequence admittance matrix of T&D system is represented as (10).

$$Y_{TD}^{0+-} = \begin{bmatrix} Y_{TD}^{00} & Y_{TD}^{0+} & Y_{TD}^{0-} \\ Y_{TD}^{+0} & Y_{TD}^{++} & Y_{TD}^{+-} \\ Y_{TD}^{-0} & Y_{TD}^{-+} & Y_{TD}^{--} \end{bmatrix} \tag{10}$$

With this developed admittance matrix, a sequence component based load flow is performed considering the unified T & D system. In this, the positive sequence is solved using the current injection iterative method, and the other sequences are solved using linear equations.

IV. Proposed SI-CPF Model

The continuation power flow (CPF) process consists of a prediction phase and a correction phase [15]. In the proposed method, the prediction step is done only for positive sequence and the corrector step is done for all sequences using a three sequence PF.

A. Three Sequence Power Flow

The generalized voltage equations of a system can be written in sequence domain as

$$\begin{bmatrix} Y^{00} & Y^{0+} & Y^{0-} \\ Y^{+0} & Y^{++} & Y^{+-} \\ Y^{-0} & Y^{-+} & Y^{--} \end{bmatrix} \begin{bmatrix} \mathbf{V}^0 \\ \mathbf{V}^+ \\ \mathbf{V}^- \end{bmatrix} = \begin{bmatrix} \mathbf{I}^0 \\ \mathbf{I}^+ \\ \mathbf{I}^- \end{bmatrix} \tag{11}$$

The values of V^+ and I^+ have higher magnitude than those of V^0, $I^0$and V^-,I^- respectively. Therefore (11) can be rewritten as three separate equations as

$$\mathbf{Y}^{00}V^0 = \mathbf{I}^0 - (Y^{0+}V^+ + Y^{0-}V^-) \tag{12}$$

$$\mathbf{Y}^{++}V^+ = \mathbf{I}^+ - (Y^{+0}V^0 + Y^{+-}V^-) \tag{13}$$

$$\mathbf{Y}^{--}V^- = \mathbf{I}^- - (Y^{-0}V^0 + Y^{-+}V^+) \tag{14}$$

Equations (12) and (14) are utilized for a linear zero sequence and negative sequence power flow respectively. Equation (13) is used for an iterative positive sequence power flow [16].

B. Proposed CPF Formulation

In the proposed CPF, the Jacobian-based gradient formation can be represented as

$$\mathbf{J}(\mathbf{x})\Delta\mathbf{x} = -g(x) \tag{15}$$

where J=$\frac{\partial g(x)}{\partial x}$ represents the Jacobian matrix. The power flow is reformulated using a loading factor λ to apply the continuation technique to the power flow problem. The generation and load variations are simulated using the following modification.

$$P^{sp} = P_0^{sp}(1+\lambda) \tag{16}$$

$$Q^{sp} = Q_0^{sp}(1+\lambda) \tag{17}$$

where $P^{sp} = P^g - P^l$ and $Q^{sp} = Q^g - Q^l$. Here P_0^{sp} and Q_0^{sp} are the total specified power of the base case where $\lambda = 0$. Therefore using loading factor λ as

$$\Delta I_i = \frac{P_{i0}^{sp}(1+\lambda) - jQ_{i0}^{sp}(1+\lambda)}{(V_i^*)} - \sum_{j=1}^{n} Y_{ji}V_j \tag{18}$$

The real and imaginary component of (18)is given by

$$\Delta I_{ri} = \frac{P_{i0}^{sp}V_{ri} + Q_{i0}^{sp}V_{mi}(1+\lambda)}{V_{ri}^2 + V_{mi}^2} - \sum_{j=1}^{N}(G_{ij}V_{rj} - B_{ij}V_{mj}) \tag{19}$$

$$\Delta I_{mi} = \frac{P_{i0}^{sp}V_{mi} - Q_{i0}^{sp}V_{ri}(1+\lambda)}{V_{ri}^2 + V_{mi}^2} - \sum_{j=1}^{N}(G_{ij}V_{mj} - B_{ij}V_{rj}) \tag{20}$$

The above current mismatch equations can be represented in a generalized form as

$$g(x,\lambda) = g(V_r, V_m, \lambda) = 0 \tag{21}$$

Linearizing (21), we have

$$dg(V_r, V_m, \lambda) = g_{V_r}dV_r + g_{V_m}dV_m + g_\lambda d\lambda = 0 \tag{22}$$

where g_λ, g_{V_m} and g_{V_r} are the derivatives of current mismatch with respect λ, V_m and V_r respectively. The real and imaginary component of g_λ can be derived as

$$g_{\lambda ri} = \frac{P_{i0}^{sp}V_{ri} + Q_{i0}^{sp}V_{mi}}{V_{ri}^2 + V_{mi}^2} = I_{ri}^{sp} \tag{23}$$

$$g_{\lambda mi} = \frac{P_{i0}^{sp}V_{mi} - Q_{i0}^{sp}V_{ri}}{V_{ri}^2 + V_{mi}^2} = I_{mi}^{sp} \tag{24}$$

$$Y_{TD}^{++} = \begin{bmatrix} y_t^{11} & y_t^{12} & y_t^{13} & 0 & 0 & 0 & 0 & 0 & 0 & 0 \\ y_t^{21} & y_t^{22}+Y^{tie1} & y_t^{23} & -Y^{tie1} & 0 & 0 & 0 & 0 & 0 & 0 \\ y_t^{31} & y_t^{32} & y_t^{33}+Y^{tie2} & 0 & 0 & 0 & 0 & -Y^{tie2} & 0 & 0 \\ 0 & -Y^{tie1} & 0 & y_{d1}^{11}+Y^{tie1} & y_{d1}^{12} & y_{d1}^{13} & y_{d1}^{14} & 0 & 0 & 0 \\ 0 & 0 & 0 & y_{d1}^{21} & y_{d1}^{22} & y_{d1}^{23} & y_{d1}^{24} & 0 & 0 & 0 \\ 0 & 0 & 0 & y_{d1}^{31} & y_{d1}^{32} & y_{d1}^{33} & y_{d1}^{34} & 0 & 0 & 0 \\ 0 & 0 & 0 & y_{d1}^{41} & y_{d1}^{42} & y_{d1}^{43} & y_{d1}^{44} & 0 & 0 & 0 \\ 0 & 0 & -Y^{tie2} & 0 & 0 & 0 & 0 & y_{d2}^{11}+Y^{tie2} & y_{d2}^{12} & y_{d2}^{13} \\ 0 & 0 & 0 & 0 & 0 & 0 & 0 & y_{d2}^{21} & y_{d2}^{22} & y_{d2}^{23} \\ 0 & 0 & 0 & 0 & 0 & 0 & 0 & y_{d2}^{31} & y_{d2}^{32} & y_{d2}^{33} \end{bmatrix} \tag{9}$$

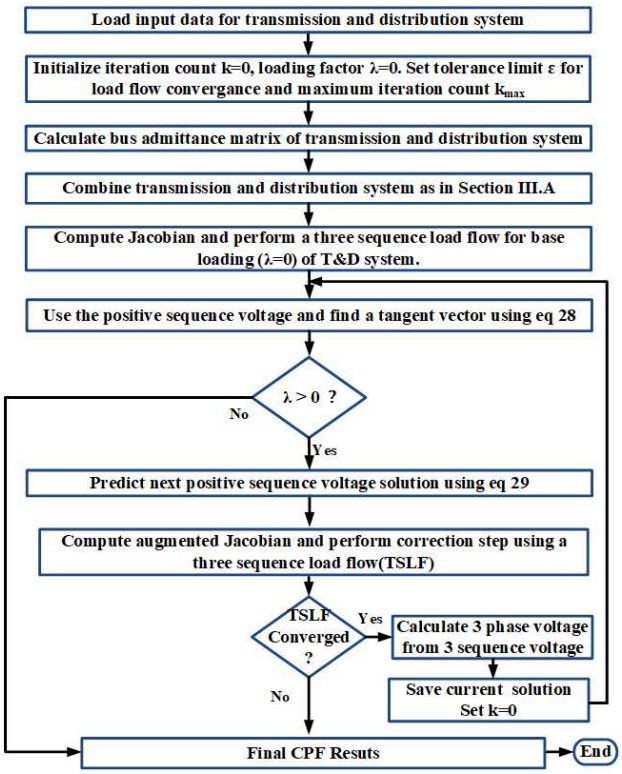

Fig. 4. Proposed Three sequence CPF.

1) Predictor Phase: The purpose of the predictor step is to estimate the next solution point. This is achieved by taking a step of an appropriate size in the direction of the tangent to the path of the solution. The first step in the prediction process is to determine a tangent vector as given by

$$\begin{bmatrix} g_{V_r} & g_{V_m} & g_\lambda \end{bmatrix} \begin{bmatrix} dV_r \\ dV_m \\ d\lambda \end{bmatrix} = 0 \tag{25}$$

In a system with m buses, the size of the tangent vector is $2m+1$ and $6m+1$ for a single-phase and three-phase system respectively. A balance between known and unknown variables is necessary to solve this equation which is achieved by introducing an extra equation. Therefore (25) can be updated as

$$\begin{bmatrix} g_{V_r} & g_{V_m} & g_\lambda \\ & E_k & \end{bmatrix} \begin{bmatrix} dV_r \\ dV_m \\ d\lambda \end{bmatrix} = \begin{bmatrix} 0 \\ \pm 1 \end{bmatrix} \tag{26}$$

The row vector E_k has zero elements for all indices except for the k^{th} index, which has a value of one. (26) can be expressed using Jacobian as

$$\begin{bmatrix} J & & g_\lambda \\ & E_k & \end{bmatrix} \begin{bmatrix} dV_r \\ dV_m \\ d\lambda \end{bmatrix} = \begin{bmatrix} 0 \\ \pm 1 \end{bmatrix} \tag{27}$$

This can be expanded as

$$\left[\begin{array}{cccc|c} \frac{\partial I_{m1}}{\partial V_{r1}} & \frac{\partial I_{m1}}{\partial V_{m1}} & \cdots & \frac{\partial I_{m1}}{\partial V_{rn}} & \frac{\partial I_{m1}}{\partial V_{mn}} & I_{m1}^{sp} \\ \frac{\partial I_{r1}}{\partial V_{r1}} & \frac{\partial I_{r1}}{\partial V_{m1}} & \cdots & \frac{\partial I_{r1}}{\partial V_{rn}} & \frac{\partial I_{r1}}{\partial V_{mn}} & I_{r1}^{sp} \\ \vdots & \vdots & \vdots & \vdots & \vdots & \\ \frac{\partial I_{mn}}{\partial V_{r1}} & \frac{\partial I_{mn}}{\partial V_{m1}} & \cdots & \frac{\partial I_{mn}}{\partial V_{rn}} & \frac{\partial I_{mn}}{\partial V_{mn}} & I_{mn}^{sp} \\ \frac{\partial I_{rn}}{\partial V_{r1}} & \frac{\partial I_{rn}}{\partial V_{m1}} & \cdots & \frac{\partial I_{rn}}{\partial V_{rn}} & \frac{\partial I_{rn}}{\partial V_{mn}} & I_{rn}^{sp} \\ \hline & & E_k & & & \end{array}\right] \begin{bmatrix} dV_{r1} \\ dV_{m1} \\ \vdots \\ dV_{rn} \\ dV_{mn} \\ d\lambda \end{bmatrix} = \begin{bmatrix} 0 \\ 0 \\ \vdots \\ 0 \\ 0 \\ \pm 1 \end{bmatrix} \tag{28}$$

The voltage and λ prediction is given by

$$\begin{bmatrix} V_r \\ V_m \\ \lambda \end{bmatrix}^{pred} = \begin{bmatrix} V_r \\ V_m \\ \lambda \end{bmatrix}^{old} + \sigma \begin{bmatrix} dV_r \\ dV_m \\ d\lambda \end{bmatrix} \tag{29}$$

where σ is a scalar that represents the step size.

2) Corrector Phase: The correction phase entails solving the augmented power flow using the solution from equation (29) as the starting point. An additional equation is introduced in the augmented power flow given by

$$\begin{bmatrix} g(x,\lambda) \\ x_k - \eta \end{bmatrix} = \begin{bmatrix} 0 \\ 0 \end{bmatrix} \tag{30}$$

where η is the predicted value of the continuation parameter x_k. The power flow equation with augmented Jacobian is given by

$$\left[\begin{array}{cccc|c} \frac{\partial I_{m1}}{\partial V_{r1}} & \frac{\partial I_{m1}}{\partial V_{m1}} & \cdots & \frac{\partial I_{m1}}{\partial V_{rn}} & \frac{\partial I_{m1}}{\partial V_{mn}} & I_{m1}^{sp} \\ \frac{\partial I_{r1}}{\partial V_{r1}} & \frac{\partial I_{r1}}{\partial V_{m1}} & \cdots & \frac{\partial I_{r1}}{\partial V_{rn}} & \frac{\partial I_{r1}}{\partial V_{mn}} & I_{r1}^{sp} \\ \vdots & \vdots & \vdots & \vdots & \vdots & \\ \frac{\partial I_{mn}}{\partial V_{r1}} & \frac{\partial I_{mn}}{\partial V_{m1}} & \cdots & \frac{\partial I_{mn}}{\partial V_{rn}} & \frac{\partial I_{mn}}{\partial V_{mn}} & I_{mn}^{sp} \\ \frac{\partial I_{rn}}{\partial V_{r1}} & \frac{\partial I_{rn}}{\partial V_{m1}} & \cdots & \frac{\partial I_{rn}}{\partial V_{rn}} & \frac{\partial I_{rn}}{\partial V_{mn}} & I_{rn}^{sp} \\ \hline & & E_k & & & \end{array}\right] \begin{bmatrix} \Delta V_{r1} \\ \Delta V_{m1} \\ \vdots \\ \Delta V_{rn} \\ \Delta V_{mn} \\ \Delta\lambda \end{bmatrix} = \begin{bmatrix} \Delta I_{m1} \\ \Delta I_{r1} \\ \vdots \\ \Delta I_{mn} \\ \Delta I_{rn} \\ 0 \end{bmatrix} \tag{31}$$

A flow chart describing steps involved in the proposed continuation power flow method is shown in Fig. 4.

V. Simulation Results

The proposed method is developed on MATLAB software using a computer with a CORE i5 processor, 6 GB RAM and

TABLE I
AVERAGE CONVERGENCE TIME

Transmission System (s)	1 Distribution System(s)	Total Time (s) (Benchmark T&D)	Total Time(s) (Unified T&D)
0.103	0.215	0.963	1.203

2.4 GHz CPU. In order to evaluate the proposed method, two test systems are developed. The first system is an integrated power grid model as shown in Fig. 5 with Transmission side modeled using IEEE 14 bus and distribution side modeled using four IEEE 123 bus test feeders. The second test system is a modified version of first T&D system where the total load on all the 3 phases of the distribution system is modified such that the net load level approximately equal the transmission system bus 14 loads on all the phases. A similar model is also developed in SIMULINK, a commercial electromagnetic transient program by modeling the IEEE 14 bus system and IEEE 123 bus test feeder used in [17] for validating the T&D test model.

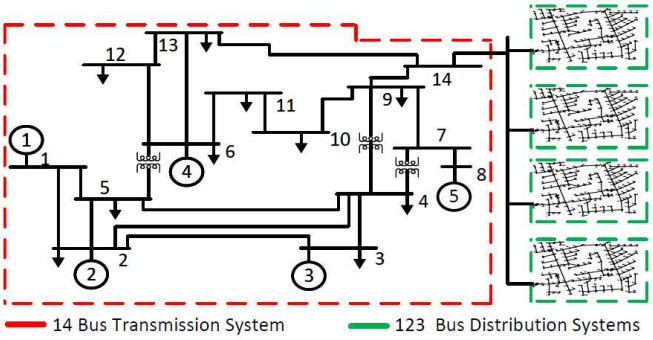

Fig. 5. Test T&D system 1 one line diagram.

A. Comparison of Proposed Sequence power flow method with state-of-the-art T&D power flow methods

The voltage magnitude obtained using proposed sequence method is compared with the state-of-the-art method discussed in [2], where the transmission side is represented in a positive sequence and the distribution side in three phase. The comparison shows that the voltage variations are very similar, as demonstrated in Fig.6. The average time for load flow convergence using the proposed method is presented in TableI.

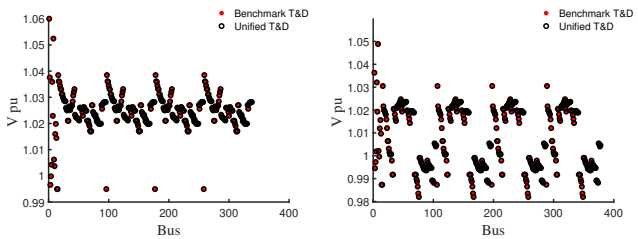

(a) B Phase (b) C Phase

Fig. 6. Voltage Magnitude with Proposed T&D PF and T&D PF in [2]

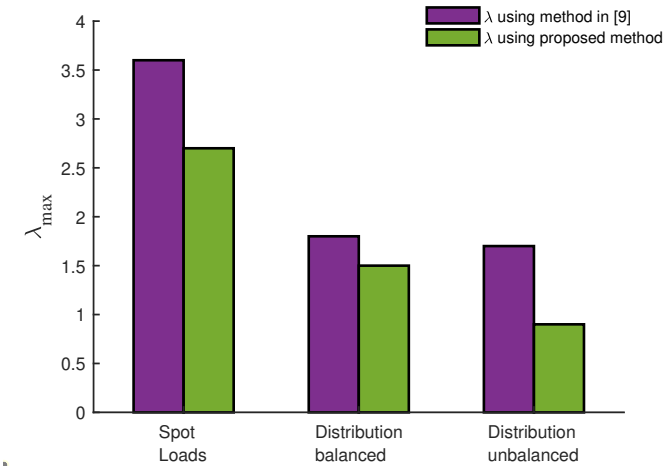

Fig. 7. Comparison of maximum loading factor.

B. Comparison of Proposed CPF with Three Sequence PF

The proposed CPF offers reduced computational demands compared to a normal power flow. This is due to the fact that, in proposed method, the initial condition for corrector step is taken from the solution of the predictor step. Table II displays the convergence iterations and computation time which shows fewer iterations for any given λ value compared to the normal three sequence PF. Moreover, while the three-sequence power flow failed for $\lambda > 0.9$ (reaching the iteration limit of 100 iterations) , the continuation power flow was successful. Hence, the proposed CPF is computationally efficient and pose superior convergence potential in comparison to the normal three-sequence power flow.

TABLE II
NUMBER OF ITERATIONS FOR LF CONVERGENCE.

λ	Sequence PF (flat start)		Proposed Sequence CPF	
	No of Iter.	T(s)	No of Iter.	T(s)
0.1	4	4.2	2	2.8
0.3	5	5.1	3	3.4
0.5	9	8.2	5	5.6
0.8	14	15.4	8	9.2
0.9	50	30	15	25.
0.921	100	50	20	32.5

C. Comparison of Proposed Sequence CPF with Positive Sequence T&D approach for VSM assessment

In this case, the voltage stability margin obtained from [9], where the transmission system is modeled as positive sequence and ution system in three phases, is compared to that obtained with proposed CPF approach for various scenarios. These scenarios include a) a transmission network connected to spot loads which represent net load of all distribution feeders, taking into account distribution system losses, b) an integrated Transmission and Distribution system with transmission side modeled in positive sequence and distribution side modeled in three phase.

The comparison results are shown in Fig. 7. It can be observed that the λ_{max} decreases drastically from 3.6 when

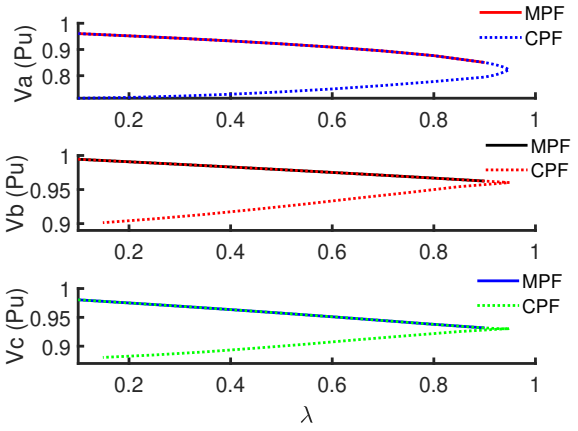

Fig. 8. Comparison of CPF and MPF.

TABLE III
SIZE OF MATRICES.

Element	Single Phase CPF	Three Phase CPF	Three Sequence CPF
Jacobian	$2p \times 2p$	$6p \times 6p$	$2m \times 2m$
Tangent Vector	$2p+1$	$6p+1$	$2p+1$
Augmented Jacobian	$2p+1 \times 2p+1$	$6p+1 \times 6p+1$	$2p+1 \times 2p+1$

spot loads are used to 1.8 in the case of positive sequence T&D approach which reduces further down to 1.5 using the proposed CPF approach where both the transmission and distribution systems are represented in three-sequence detail. It is also evident that there is a reduction in λ_{max} when an unbalanced system is used over the balanced system. The reduction is from 1.5 to 0.9 using the proposed three-sequence CPF method, and from 1.8 to 1.6 using the VSM T&D method in [9]. Therefore, the proposed approach captures the impact of distribution system unbalance on the VSM more prominently.

D. Comparison of Proposed Three Sequence CPF with Three phase CPF for VSM assessment

Comparisons of the proposed architecture with a multi-period power flow are illustrated in Fig. 8. It can be seen that the proposed method provides accurate voltage stability limits. For a system with p buses, the Jacobian size in any three-phase power flow method will be 6p x 6p. However, in the case of a three-sequence approach, the Jacobian size will be 2p x 2p for the positive sequence sub-problem and p x p for the two sets of linear simultaneous equations representing the negative and zero sequence sub-problems. As a result, the computational load associated with the proposed three sequence approach is notably reduced when compared to the three-phase method. A comparison of the sizes of different matrices including the Jacobian, augmented Jacobian and prediction tangent is shown in Table III.

VI. CONCLUSION AND FUTURE WORK

This paper introduces a novel continuation power flow technique tailored for integrated transmission and distribution systems. This method effectively examines the power grid's voltage stability while considering imbalances in the grid and loads, various load types, and fluctuations in renewable energy sources. The proposed three-sequence approach has significantly lower computational burden in contrast to the three phase method. The outcomes demonstrate the efficacy and precision of the suggested CPF model in assessing the power grid's weak phase voltage stability margin. Future works will involve incorporating Distributed Energy Resources (DERs), voltage regulator controls, and scalability testing with larger transmission and distribution systems.

REFERENCES

[1] M. A. I. Khan, A. Suresh, S. Paudyal, and S. Kamalasadan, "Decoupled and unified approaches for solving transmission and distribution co-simulations," in *2019 North American Power Symposium (NAPS)*, 2019.

[2] Q. Huang and V. Vittal, "Integrated transmission and distribution system power flow and dynamic simulation using mixed three-sequence/three-phase modeling," *IEEE Transactions on Power Systems*, vol. 32, no. 5, pp. 3704–3714, Sept 2017.

[3] R. Venkatraman, S. K. Khaitan, and V. Ajjarapu, "A combined transmission-distribution system dynamic model with grid-connected dg inverter," in *2017 IEEE Power Energy Society General Meeting*, July 2017, pp. 1–5.

[4] H. Jain, B. Palmintier, I. Krad, and D. Krishnamurthy, "Studying the impact of distributed solar pv on power systems using integrated transmission and distribution models," in *2018 IEEE/PES Transmission and Distribution Conference and Exposition (T D)*, April 2018, pp. 1–5.

[5] B. Palmintier, E. Hale, T. Hansen, W. Jones, D. Biagioni, K. Baker, H. Wu, J. Giraldez, H. Sorensen, M. Lunacek, N. Merket, J. Jorgenson, and B.-M. Hodge, "Integrated distribution-transmission analysis for very high penetration solar pv (final technical report)," 01 2016.

[6] P.Evans, "Integrated transmission and distribution model for assessment of distributed wholesale photovoltaic generation," 4 2013.

[7] M. Dilek, F. de Leon, R. Broadwater, and S. Lee, "A robust multiphase power flow for general distribution networks," *IEEE Transactions on Power Systems*, vol. 25, no. 2, pp. 760–768, May 2010.

[8] B. Palmintier, D. Krishnamurthy, P. Top, S. Smith, J. Daily, and J. Fuller, "Design of the helics high-performance transmission-distribution-communication-market co-simulation framework," in *2017 Workshop on Modeling and Simulation of Cyber-Physical Energy Systems (MSCPES)*, April 2017, pp. 1–6.

[9] A. K. Bharati and V. Ajjarapu, "Investigation of relevant distribution system representation with dg for voltage stability margin assessment," *IEEE Transactions on Power Systems*, vol. 35, no. 3, 2020.

[10] A. Singhal and V. Ajjarapu, "Long-term voltage stability assessment of an integrated transmission distribution system," in *2017 North American Power Symposium (NAPS)*, 2017, pp. 1–6.

[11] A. Suresh, S. Kamalasadan, and S. Paudyal, "A novel three-phase transmission and unbalance distribution co-simulation power flow model for long term voltage stability margin assessment," in *2021 IEEE Power Energy Society General Meeting (PESGM)*, 2021, pp. 1–5.

[12] R. Maharjan and S. Kamalasadan, "A new approach for voltage control area identification based on reactive power sensitivities," in *2015 North American Power Symposium (NAPS)*. IEEE, 2015, pp. 1–6.

[13] P. S. Nirbhavane, L. Corson, S. M. H. Rizvi, and A. K. Srivastava, "Tpcpf: Three-phase continuation power flow tool for voltage stability assessment of distribution networks with distributed energy resources," *IEEE Transactions on Industry Applications*, vol. 57, no. 5, pp. 5425–5436, 2021.

[14] A. Suresh, K. Murari, and S. Kamalasadan, "Injected current sensitivity based load flow algorithm for multi-phase distribution system in the presence of distributed energy resource," *IEEE Transactions on Power Delivery*, pp. 1–1, 2022.

[15] V. Ajjarapu and C. Christy, "The continuation power flow: a tool for steady state voltage stability analysis," *IEEE Transactions on Power Systems*, vol. 7, no. 1, pp. 416–423, 1992.

[16] K. L. Lo and C. Zhang, "Decomposed three-phase power flow solution using the sequence component frame," *IEE Proceedings C - Generation, Transmission and Distribution*, vol. 140, no. 3, pp. 181–188, 1993.

[17] A. Suresh, R. Bisht, and S. Kamalasadan, "A coordinated control architecture with inverter-based resources and legacy controllers of power distribution system for voltage profile balance," *IEEE Transactions on Industry Applications*, vol. 58, no. 5, pp. 6701–6712, 2022.